The *Xenopus tropicalis* orthologue of TRPV3 is heat sensitive

Beiying Liu and Feng Qin

Department of Physiology and Biophysical Sciences, State University of New York at Buffalo, Buffalo, NY 14214

Thermosensitive members of the transient receptor potential (TRP) family of ion channels (thermal TRP channels) play a crucial role in mammalian temperature sensing. Orthologues of these channels are present in lower vertebrates and, remarkably, some thermal TRP orthologues from different species appear to mediate opposing responses to temperature. For example, whereas the mammalian TRPV3 channel is activated by heat, frog TRPV3 is reportedly activated by cold. Intrigued by the potential implications of these opposing responses to temperature for the mechanism of temperature-dependent gating, we cloned *Xenopus laevis* TRPV3 and functionally expressed it in both mammalian cell lines and *Xenopus* oocytes. We found that, when expressed in mammalian cells, the recombinant channel lacks the reported cold sensitivity; rather, it is activated by temperatures >50°C. Furthermore, when expressed in mammalian cells, the frog orthologue shows other features characteristic of mammalian TRPV3, including activation by the agonist 2-aminoethoxydiphenyl borate and an increased response with repeated stimulation. We detected both heat- and cold-activated currents in *Xenopus* oocytes expressing the recombinant frog TRPV3 channel. However, cold-activated currents were also apparent in control oocytes lacking recombinant TRPV3. Our data indicate that frog TRPV3 resembles its mammalian orthologues in terms of its thermosensitivity and is intrinsically activated by heat. Thus, all known vanilloid receptors are activated by heat. Our data also show that *Xenopus* oocytes contain endogenous receptors that are activated by cold, and suggest that cold sensitivity of TRP channels established using *Xenopus* oocytes as a functional expression system may need to be revisited.

The Journal of General Physiology

INTRODUCTION

Sensation of temperature is a basic function required by an organism for survival and adaptation. In mammals, the detection of temperature involves specialized sensory neurons that innervate skin and other terminal organs. The myelinated Aδ fibers have a role in cold reception, whereas the unmyelinated C fibers mediate responses for warmth and noxious temperature sensation (Spray, 1986). Warming causes an increase of the firing rates of action potentials in warmth receptors, whereas cooling results in increases in the rates of cold receptors. The changes of action potentials are relayed by the neurons from the peripheral nerve system to the central nerve system where they are interpreted as distinct thermal sensations.

The initial transduction of temperature changes has been thought to involve temperature-sensitive ion channels on nerve endings. Several members from the transient receptor potential (TRP) ion channel family are found to be gated by heat or cold at different, physiologically relevant temperature ranges. TRPV1–4 from the vanilloid subfamily are activated by heat in the warm and noxious hot ranges (Caterina et al., 1997, 1999; Peier et al., 2002b; Smith et al., 2002; Watanabe et al., 2002; Xu et al., 2002). TRPM8 from the melastatin subfamily is activated by cold <22°C (McKemy et al., 2002; Peier et al., 2002a). Thermal channels are also responsive to other stimuli, especially natural plant products known to mimic temperature sensation. Capsaicin, the hot ingredient of chili peppers, activates TRPV1 (Caterina et al., 1997). Monoterpene compounds like carvacrol, thymol, and eugenol, the warmth-producing flavors, have effects on TRPV3 (Xu et al., 2006). Menthol from mint oil, a major source for cool sensation, is a strong agonist of TRPM8 (McKemy et al., 2002). Thus, the activation of different thermal TRP channels is correlated with the distinct hot and cold sensations. Gene knockout experiments confirm that animals lacking functional thermal TRP channels are impaired in normal detection of temperature as well as in thermal hyperalgesia (Caterina et al., 2000; Davis et al., 2000; Moqrich et al., 2005; Bautista et al., 2007; Dhaka et al., 2007), which further support the essential roles of these TRP channels in thermal sensation.

Thermal TRP channels are also found in lower vertebrates and invertebrates. The TRPA1 gene has been identified in snakes (Gracheva et al., 2010), fruit fly (Viswanath et al., 2003), fish (Prober et al., 2008), and worms (Kindt et al., 2007), where its function is correlated with thermotaxis behaviors in many organisms. TRPV1 and TRPV3 have also been reported in lower

Correspondence to Feng Qin: qin@buffalo.edu

Abbreviations used in this paper: 2-APB, 2-aminoethoxydiphenyl borate; RR, ruthenium red; TRP, transient receptor potential.

The Rockefeller University Press $30.00
J. Gen. Physiol. Vol. 146 No. 5 411–421
www.jgp.org/cgi/doi/10.1085/jgp.201511454

vertebrates such as fish and frogs (Saito et al., 2011; Ohkita et al., 2012; Gau et al., 2013; Majhi et al., 2013). Notably, the nonmammalian orthologues can differ substantially from their mammalian counterparts in activation profiles, some of which appear to even develop opposite thermal sensitivity (Viswanath et al., 2003; Saito et al., 2011). For example, whereas the mammalian TRPV3 is activated by heat, its frog orthologue in *Xenopus tropicalis* (western clawed frog) reportedly responds to cold with a temperature activation threshold <16°C. Thus, the channel has been suggested to mediate nociceptive cold sensation instead of heat sensation in frogs (Saito et al., 2011).

It is seemingly paradoxical that a channel can be heat sensitive in one species but cold sensitive in another. In theory, there are possibilities that a channel can be activated by both heat and cold. For example, the recently proposed heat capacity model suggests that the temperature sensitivity of thermal channels results from a heat capacity change during opening (Clapham and Miller, 2011). Large heat capacity changes are normally associated with changes in solvation states of hydrophobic residues, which, like the aqueous solubility of hydrocarbons, can be promoted by both heating and cooling. Thus, the heat capacity model predicts that thermal channels possess dual hot and cold sensitivity (Chowdhury et al., 2014). Alternatively, the directionality of temperature activation of a channel may also be encoded by the allosteric linkage that transduces thermal energy to the gate (Jara-Oseguera and Islas, 2013). The allosteric linkage can have a temperature dependence to either promote or inhibit channel opening, thereby making the channel sensitive to the direction of temperature changes. Presently, these models still lack direct experimental support (Qin, 2013). The study of the opposite temperature sensitivity of homologous thermal channels could provide an opportunity to experimentally elucidate these models and the principles of temperature gating of thermal channels in general.

The frog TRPV3, if its cold sensitivity is proven, could serve as a good model for studying the opposite temperature sensitivity of thermal channels, as the heat sensitivity of its mammalian counterparts has been firmly established and extensively investigated. However, the previous experiment demonstrating the cold sensitivity of frog TRPV3 was based on electrophysiological recording in whole oocytes. Whether the channel is intrinsically cold sensitive or acquires its apparent cold sensitivity from other cold-sensitive regulatory elements remains uncertain. Thus, we have decided to resolve these issues by comparing the channel activity in different experimental settings in conjunction with the use of fast-temperature clamp to expose thermal sensitivity at high temperature ranges that had not been probed previously.

MATERIALS AND METHODS

Cloning of *Xenopus tropicalis* TRPV3 gene

Xenopus tropicalis frogs were purchased from Xenopus Express, Inc. Quick-RNA MicroPrep (Zymo Research) was used for total RNA extraction. A small piece of skin of the frog was extracted from the legs and dissolved in the RNA lysis buffer. The tissue was homogenized and then centrifuged at a low speed to remove debris. The supernatant was transferred to a spin column (Zymo Research) for purification of RNA. The integrity of the resulting total RNA was tested on the basis of the quality of 28S and 18S rRNA bands on a 1% agarose gel. Reverse transcription from the eluded total RNA was performed with the SuperScript First-Strand Synthesis System for RT-PCR (Invitrogen) according to the manufacturer's protocol. About 2.5 µl of products was used for the PCR reaction, with primers designed to amplify the coding sequence of the TRPV3 transcript. The PCR product was subcloned into the pIRES2-EGFP expression vector (Invitrogen) and was verified by full-length sequencing.

Cell culture and expression

HEK293 cells were grown in Dulbecco's modified Eagle's medium containing 10% fetal bovine serum (Hyclone Laboratories, Inc.) and 1% penicillin/streptomycin and were incubated at 37°C in a humidified incubator gassed with 5% CO_2. Transfection was made at a confluence of ∼80% by calcium phosphate precipitation. Monomeric red fluorescent protein (mRFP) was cotransfected for laser beam positioning. Experiments took place usually 10–28 h after transfection.

Electrophysiology

Patch-clamp recording was made in whole-cell and excised-patch configurations. Currents were amplified using an amplifier (Axopatch 200B; Axon Instruments), low-pass filtered at 5–10 kHz through the built-in eight-pole Bessel filter, and sampled at 10–20 kHz with a multifunctional data acquisition card (National Instruments). Data acquisition was controlled by custom-made software, which was capable of synchronous I/O and simultaneous control of laser and patch-clamp amplifier. Patch pipettes were fabricated from borosilicate glass capillaries (Sutter Instrument) and fire-polished to a resistance of <5 MΩ when filled with 150 mM of CsCl solution. Pipette series resistance and capacitance were compensated using the built-in circuitry of the amplifier (50–70%), and the liquid-junction potential between the pipette and bath solutions was zeroed before seal formation. Currents were evoked from a holding potential of −60 mV. Measurements were expressed as mean ± SEM.

Bath solutions for whole-cell recording consisted of (mM): 150 NaCl, 5 EGTA, and 10 HEPES, pH 7.4 (adjusted with NaOH). Electrodes were filled with (mM): 140 CsCl, 10 HEPES, and 1 EGTA, pH 7.4 (adjusted with CsOH). For excised patches, symmetric solutions of 150 NaCl were used.

Temperature jump

Fast-temperature jumps were produced by the laser irradiation approach as described previously (Yao et al., 2009). In brief, laser emission from a single-emitter infrared high power laser diode was launched into a multimode fiber with a 100-µm core diameter and 0.2 NA. The other end of the fiber was positioned close to cells as the perfusion pipette normally was. The laser diode was driven by a pulsed quasi-CW current power supply (Lumina Power). Pulsing was controlled from a computer through the data acquisition card using a custom program. A green laser line (532 nm) was coupled to the fiber to aid alignment. The beam spot on the coverslip was identified by illumination of mRFP-expressing cells.

Constant temperature steps were generated by irradiating the tip of an open pipette and using the current of the electrode as the readout for feedback control. The laser was first powered on for a brief duration (<0.75 ms) to reach the target temperature, and was subsequently modulated to maintain a constant pipette current. The sequence of the modulation pulses was stored and subsequently played back to apply temperature jumps to whole cells or membrane patches. Temperature was calibrated offline from the pipette current using the temperature dependence of electrolyte conductivity.

Xenopus laevis oocyte preparation and recording

Defolliculated stage V–VI *Xenopus* oocytes were obtained from Ecocyte Bioscience. Injection of western clawed frog TRPV3 cRNA took place on the same day of arrival. Experiments were performed 3–7 d after injection. Whole-cell currents were measured with an amplifier (OC-725C; Warner Instrument) using the two-electrode voltage-clamp technique. Electrodes were pulled from borosilicate glass capillaries and filled with 3 M of KCl solution. When immersed in perfusion buffer, the current electrode had a resistance of ~0.4–2 MΩ, whereas the voltage electrode had a resistance of 0.4–10 MΩ. Oocytes were clamped at a holding voltage of −60 mV. Bath and wash solutions were the same as ND96, except that no Ca^{2+} was added. The agonist and antagonist were diluted to the wash solution and applied to oocytes by perfusion. For cooling/heating experiments, the wash solution was precooled/heated and then applied by perfusion. Measurements were expressed as mean ± SEM.

RESULTS

Cloning of frog TRPV3

The full-length cDNA of *Xenopus tropicalis* TRPV3 was cloned by RT-PCR using total RNA extract from the toe

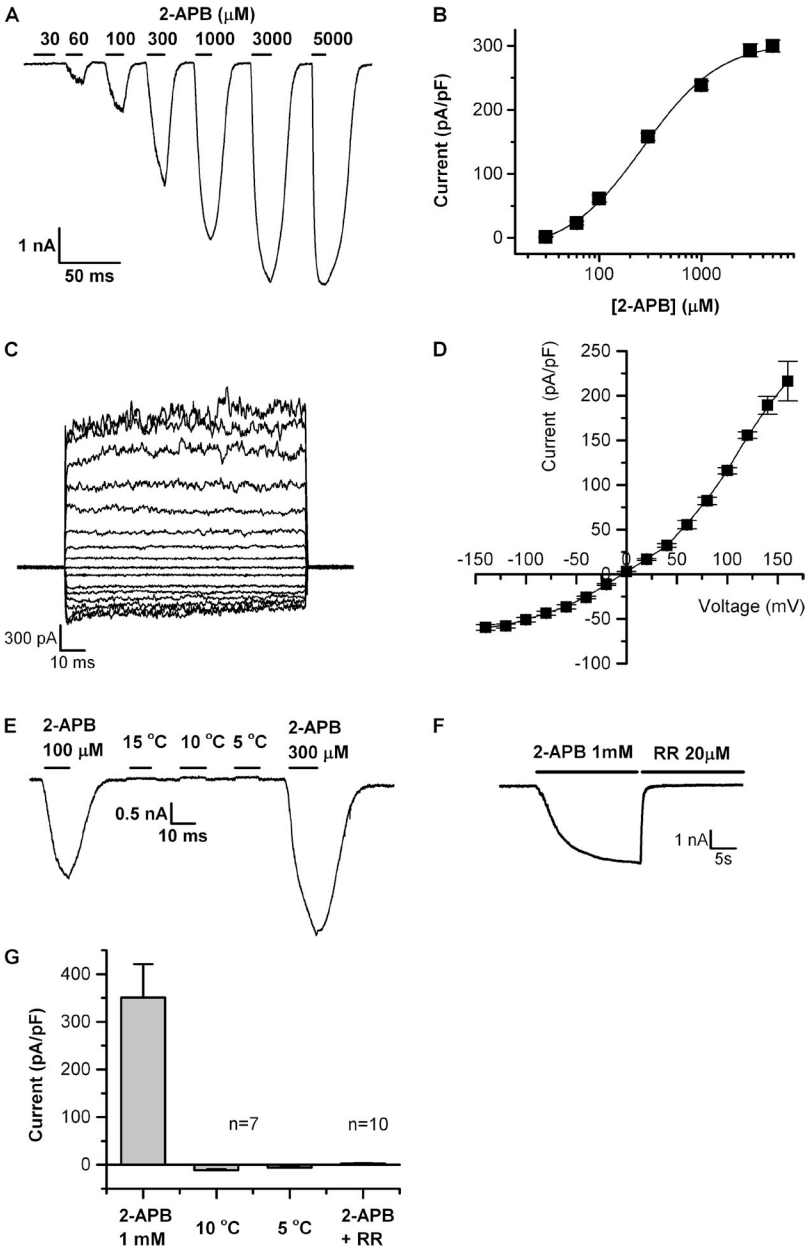

Figure 1. Frog TRPV3 is activated by 2-APB, but not by cold, in HEK293 cells. (A) Representative 2-APB–evoked currents in HEK293 cells expressing frog TRPV3. Holding potential, −60 mV. (B) Dose–response curve of 2-APB. The current density normalized by membrane capacity is shown. The solid line represents a fit by a Hill equation, with I_{max} = 330 ± 14 pA/pF, n_H = 1.15 ± 0.14, and EC_{50} = 269 ± 28 μM (n = 11). (C and D) Voltage dependence of 2-APB response, showing that the current was outwardly rectified. [2-APB] = 500 μM. n = 5 for current–voltage relationship. (E) Cold evoked no activity in HEK293 cells expressing frog TRPV3, whereas 2-APB produced robust currents before or after cooling in the same cells. Holding potential, −60 mV. (F) Responses evoked by 2-APB were rapidly inhibited by 20 μM RR. (G) Statistic plot of cold responses versus 2-APB responses recorded from the same cells (n = 7). The small decrease in the current upon cooling reflected changes in the baseline activity. Also plotted is the residual 2-APB response after the application of RR, showing the potent inhibition of the current by RR (20 μM RR and 1 mM 2-APB; n = 10). All recordings except cold responses were at room temperature. Error bars represent mean ± SEM.

of the western clawed frog. The resulting cDNA sequence was the same as previously published (Saito et al., 2011). The gene was subcloned into a mammalian expression vector (pIRES2) for functional expression in mammalian cells. We found that the cloned channel was well expressed in HEK293 cells (see current recordings below), so we have focused our functional experiments first in the HEK293 cell line.

Frog TRPV3 is activated by 2-aminoethoxydiphenyl borate (2-APB), but not by cold

2-APB is a common agonist for both mammalian TRPV3 and frog TRPV3. Thus, we first tested the 2-APB sensitivity of the recombinant frog TRPV3. As illustrated in Fig. 1, the channel indeed showed robust responses to 2-APB in a concentration-dependent manner. A detectable response was seen at 60 µM, and the response tended to saturate above 3 mM. This responsiveness range appears to be higher than that of the mammalian TRPV3 (Liu et al., 2011), but it is consistent with that previously reported for frog TRPV3 expressed in *Xenopus* oocytes (Saito et al., 2011). Fig. 1 B plots the dose–response curve of the 2-APB activation. The plot was fit by a Hill equation, with Hill coefficient $n_H = 1.15 \pm 0.14$ and $EC_{50} = 269 \pm 28$ µM ($n = 11$). As to be seen later, the gating of the channel was not at equilibrium; thus, the fitted parameters were phonological values for the apparent responses. Also in agreement with the previous report (Saito et al., 2011), the 2-APB response in HEK293 cells was voltage dependent. Fig. 1 C shows representative recordings of 2-APB–evoked currents at different voltages. The resulting current–voltage relationship was similarly outward rectified as it was when expressed in *Xenopus* oocytes (Fig. 1 D).

Although the 2-APB response of the cloned frog TRPV3 was similar to that reported previously, we further tested the cold sensitivity of the recombinant channel. However, lowering ambient temperature to 15°C, which was below the reported temperature threshold for cold activation in *Xenopus* oocytes, produced no detectable response in HEK293 cells expressing the recombinant channel (Fig. 1 E). This absence of activity

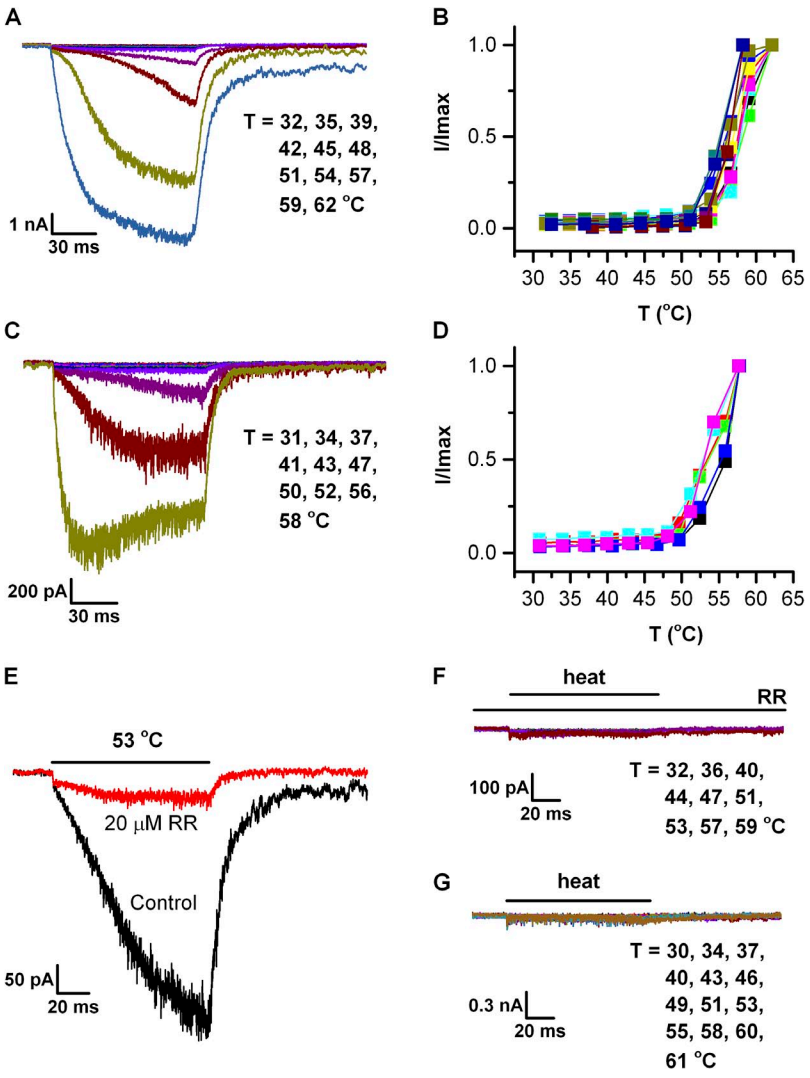

Figure 2. Frog TRPV3 is heat sensitive. (A) Representative whole-cell current evoked by temperature jumps in a frog TRPV3–expressing HEK293 cell. Each temperature pulse was 100 ms in duration. The rise time was <0.75 ms. Significant heat-sensitive activity started to occur at 51–54°C. (B) Temperature-response profiles derived from individual recordings (n = 14). Currents were normalized by their maximum responses, respectively. (C and D) Similar responses recorded from excised membrane patches in the outside-out configuration (n = 6). (E) Heat-evoked currents were suppressed by 20 µM RR. Currents in outside-out patches were elicited with a temperature jump to 53°C. RR was applied to patches by perfusion between temperature jumps. The application of RR suppressed the initial current by 94 ± 2% (n = 5). (F) Pre-application of RR to the bath solution prevented activation of heat-sensitive current. Temperature jumps ranging from 32 to 59°C were applied. Representative traces from six recordings. (G) Temperature responses from untransfected control HEK293 cells. Temperature jumps in the range of 30 to 61°C produced no detectable heat response. Representative traces for >10 recordings. Holding potential of −60 mV for all recordings.

was not caused by insufficient cooling. Further decreasing the temperature to 10 or 5°C still did not evoke a detectable current (Fig. 1 E). Instead, cooling caused an upshift in the baseline, which was presumably because of a decrease in the leak current. In these cells (showing no cold activity), the application of 2-APB, either before or after cold stimulation, however, could elicit a robust response (Fig. 1 E). Thus, the insensitivity to cold in these cells was not caused by the lack of expression of functional channels. Moreover, the current evoked by 2-APB could be rapidly inhibited by 20 mM ruthenium red (RR), a common pore blocker of vanilloid receptors (Fig. 1, F and G), further supporting the observation that the current evoked by 2-APB was indeed mediated by the heterologously expressed frog TRPV3. In all tested cells with 2-APB responses ($n > 10$), none exhibited a cold-sensitive current (Fig. 1 G). Thus, our data suggest that the cloned channel is functional when expressed in HEK293 cells, but it is not sensitive to cold under our experimental conditions.

Frog TRPV3 is heat sensitive

Because the mammalian TRPV3 is heat sensitive, we tested whether heat could also activate frog TRPV3. Fig. 2 A shows representative current traces elicited by temperature jumps in HEK293 cells transiently transfected with frog TRPV3. No significant activity was observed at temperatures <51°C. But when the temperature was >54°C, it resulted in a robust, rapidly increasing response. Fig. 2 B plots the temperature-response profile of the current. The current shows a steep temperature dependence above ~54°C, which was clearly distinct from the baseline current. The Arrhenius plot of the relationship had a slope corresponding to an activation enthalpy of 93 ± 7 kcal/mol ($n = 14$) or an equivalent Q_{10} of ~71 at 54°C.

To draw insights on whether the heat sensitivity in whole cells is intrinsic to the channel, we performed parallel recordings in excised membrane patches. As shown in Fig. 2 C, heat remained to evoke a robust activity in membrane patches (outside-out). The activation seemed to be faster in patches than in intact cells. But the basic heat sensitivity including the temperature threshold of activation (50–55°C) and the steep temperature dependence are analogous to those in whole cells (Fig. 2 D). Quantitatively, the heat response in patches had a slope sensitivity equivalent to an activation enthalpy of 83 ± 6 kcal/mol ($n = 6$), which was slightly lower than but still in the range of the energetic obtained from whole cells. The strong temperature dependence of the heat response is thus independent of the patch configuration, indicating that it is membrane delimited.

To further address whether the heat response resulted from heterologously expressed frog TRPV3, we examined the sensitivity of the current to RR. In one test, we applied 20 μM RR to patches by perfusion. Although heat evoked a profound response before the treatment with RR, the same temperature jump applied immediately after the perfusion produced only a miniature response (Fig. 2 E). On average, the heat response was suppressed by 94 ± 2% ($n = 5$) after the RR application. In another test, we included 20 μM RR directly in the bath solution. As shown in Fig. 2 F, the pre-application of RR nearly fully inhibited heat responses. In cells that were not transfected with frog TRPV3, temperature jumps up to 61°C also evoked no detectable temperature response ($n > 10$) at a hyperpolarization potential (Fig. 2 G). Collectively, these experiments indicate that our measured heat activity was indeed caused by the heterogeneously expressed frog

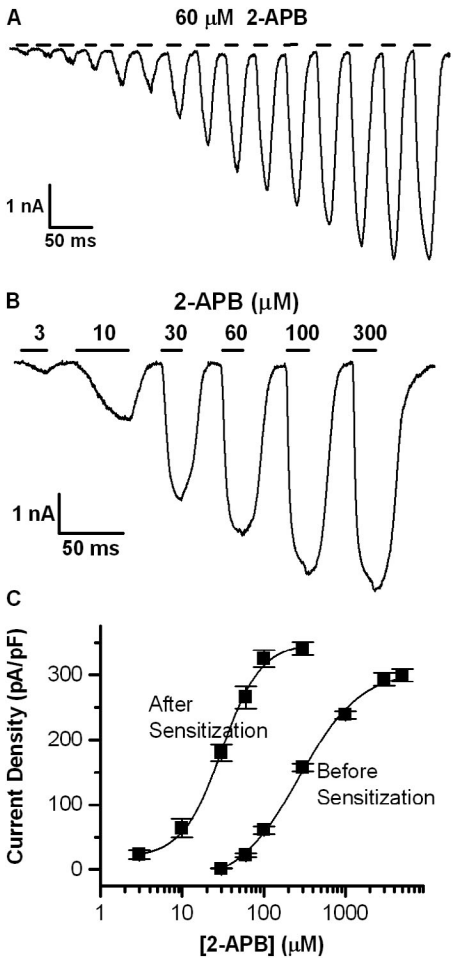

Figure 3. Sensitization of frog TRPV3 by 2-APB. (A) Repetitive 2-APB responses at the same concentration (60 μM), recorded from frog TRPV3–expressing HEK293 cells. The current was increased progressively with repeated stimulations. Representative traces from 11 cells. (B and C) Concentration dependence of frog TRPV3 after sensitization. Solid lines in C are fits to the Hill equation ($I_{max} = 330 \pm 10$ pA/pF, $n_H = 1.8 \pm 0.26$, and $EC_{50} = 31 \pm 2$ μM; $n = 10$). Also shown in C is the dose–response curve before sensitization. Error bars represent mean ± SEM.

TRPV3. The channel is activated by heat and possesses a strong temperature dependence.

Sensitization of agonist activation

The responsiveness to 2-ABP and heat of frog TRPV3 suggests that the channel has similar activation properties to its mammalian orthologues. Another distinct feature of TRPV3 is that its gating undergoes strong hysteresis (Liu et al., 2011), a process also known as sensitization. To further compare frog TRPV3 with its mammalian orthologues, we examined whether the gating of frog TRPV3 also involves hysteresis. We first tested its activation by 2-APB. Fig. 3 A illustrates repetitive responses of frog TRPV3 evoked by 2-APB at the same concentration (60 µM). The current was small initially. But it was increased progressively over subsequent stimulations, although the concentration of the agonist remained unchanged. Eventually, after ∼14 repeated stimulations, the current was reaching a steady state, suggesting that the gating could eventually become reversible. This use-dependent sensitization of the agonist response is a hallmark feature of mammalian TRPV3, which occurs as a consequence of hysteresis of gating. Thus, the experiment indicates that frog TRPV3 also involves hysteretic gating as its mammalian orthologues.

To quantify the change of sensitivity, we measured the dose–response curves of frog TRPV3 before and after sensitization. Fig. 3 B shows the sensitized 2-APB responses over a series of 2-APB concentrations. A concentration of 3 µM was able to evoke a response after sensitization, and the response could approach saturation at a concentration as low as ∼100 µM. These concentrations were 20–30 times lower than those before sensitization. Fig. 3 C compares the dose–response relationships before and after sensitization. The dose–response curve was profoundly leftward-shifted after sensitization, with EC_{50} being reduced to 31 µM from 269 µM. As compared with the profound change in EC_{50}, the changes in the steepness of the curve and the maximum response appeared to be secondary (Hill coefficient, n_H = 1.8 ± 0.3; current density, I_{max} = 330 ± 10 pA/pF; n = 10). Thus, the hysteresis of gating has an impact mainly on the EC_{50} of agonist sensitivity of the channel.

Hysteresis of heat activation

We next examined whether the heat activation of frog TRPV3 also undergoes hysteresis. In these experiments, we measured heat responses of the channel in the same cells to a family of temperature jumps (32–62°C) applied consecutively. Fig. 4 (A and B) illustrates such responses recorded in the same cell. Indeed, the activation of the channel between the first and the second run changed dramatically in both kinetics and temperature dependence. In the first run of stimulation (Fig. 4 A), the heat response exhibited a high temperature threshold where a detectable current was seen only >54°C. Once above the threshold, both current amplitude and activation time course were increased rapidly with temperature. During the second run of stimulation by the same temperature jumps (Fig. 4 B), the channel appeared to become responsive even at warm temperatures, indicating that the temperature threshold of activation was profoundly reduced. The current response also tended to increase more evenly with temperature, suggesting that the temperature dependence of the response was also decreased. Fig. 4 C confirms that the current–temperature relationship resulting from the second run had lower slope sensitivity than the first run. The energetic of the activation as estimated from the Arrhenius plot of the relationship was ∼19 ± 2 kcal/mol (n = 5), suggesting that the channel began to have only a nominal temperature dependence. Unlike the change in slope sensitivity, the change in the maximal current at 62°C was negligible (Fig. 4 D). These data

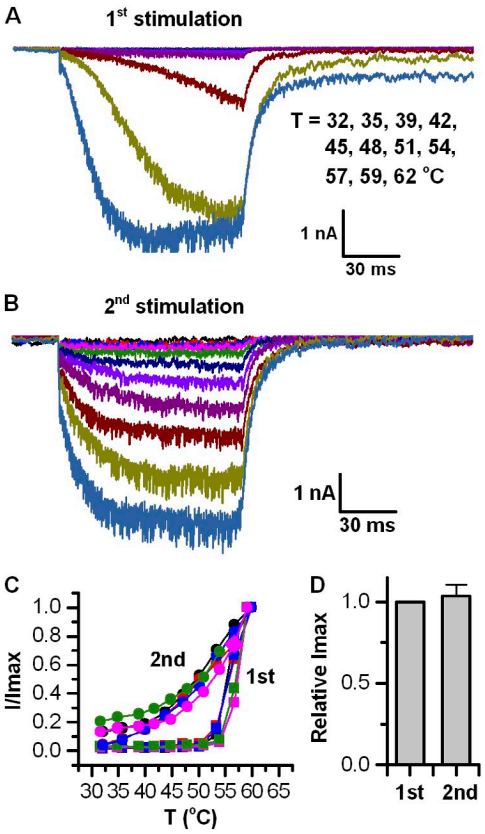

Figure 4. Hysteresis of heat activation in frog TRPV3. (A) Current responses upon initial heat stimulation. Each temperature pulse was 100 ms. (B) Current responses to the second stimulation from the same cell. The same temperature jumps were used for both stimulations. (C) Temperature-response profiles before and after hysteresis. Responses from the same cells for the first and the second stimulation are shown (n = 5). (D) Relative change of the maximum response between the first and the second run (n = 5). Recordings were from HEK293 cells at −60 mV. Error bars represent mean ± SEM.

suggest that the heat activation of frog TRPV3 possesses similar hysteresis properties to the agonist response. Overall, the frog TRPV3 resembles its mammalian orthologues in basic biophysical gating properties including heat sensitivity.

Temperature sensitivity of TRPV3 in *Xenopus* oocytes

Our failure to detect cold sensitivity of frog TRPV3 in mammalian cells could occur if the thermal sensitivity of the channel is dependent on cell types. To determine whether this was the reason, we examined its cold activity directly in *Xenopus* oocytes. As reported previously (Saito et al., 2011), both cold and 500 mM 2-APB could evoke a current in oocytes injected with TRPV3 cRNA (Fig. 5 A). On average, the current evoked by 2-APB was 1.88 ± 0.33 µA (n = 13), whereas the cold response was 3.38 ± 0.46 µA (n = 22). However, the cold- and 2-APB–sensitive currents exhibited distinct characteristics. The cold-sensitive current was rapidly inactivated, whereas the 2-APB response was sustained (buffers contained nominal Ca^{2+}). The cold activation typically occurred at temperatures <20°C. However, the threshold of the

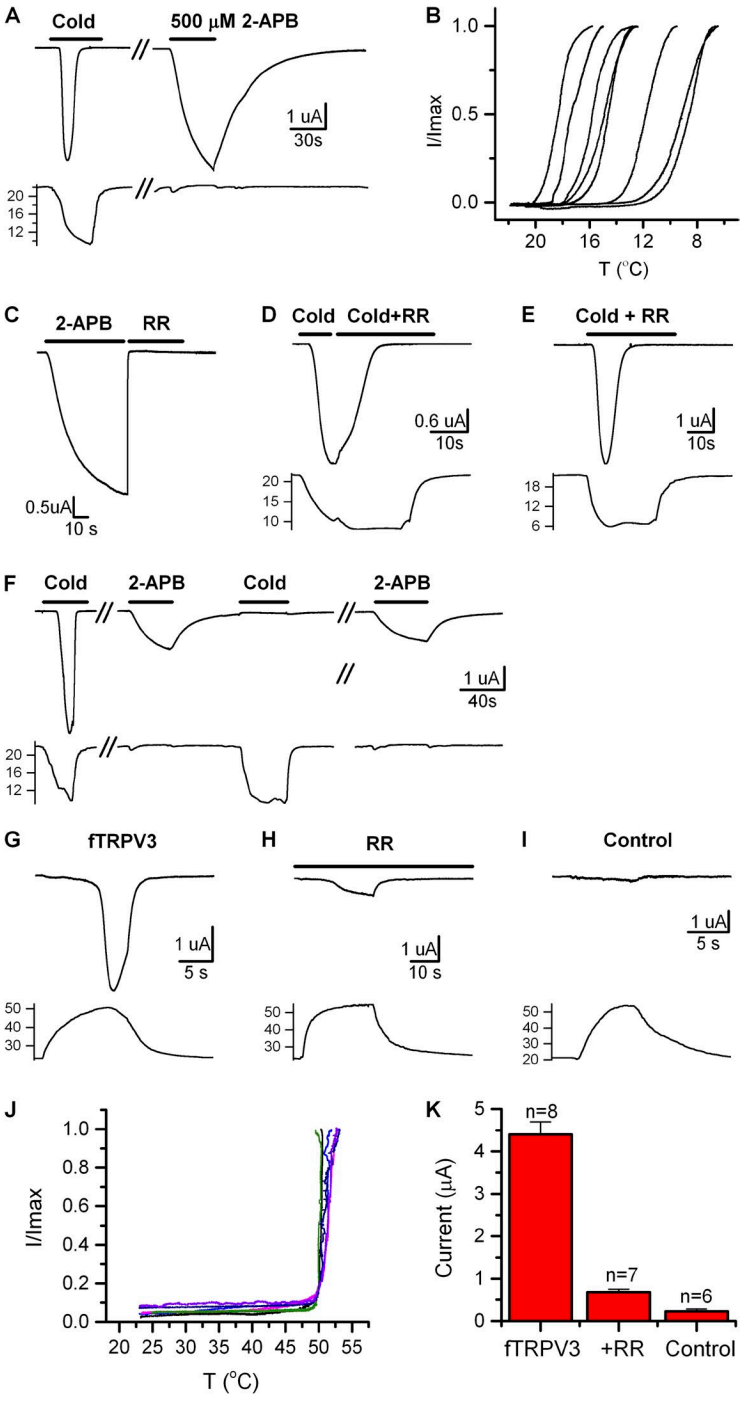

Figure 5. 2-APB and cold responses in frog TRPV3–expressing *Xenopus* oocytes. (A) Cold and 500 µM 2-APB both evoked currents in frog TRPV3–injected *Xenopus* oocytes. Bottom trace plots bath temperature change in time. (B) Representative cold-response profiles from 10 oocytes. The temperature activation threshold was variable from around 20 to 12°C. Currents were normalized to their peak values. Responses during the cooling phase are shown. (C) 2-APB–dependent current was rapidly blocked by 20 µM RR. (D) Cold-evoked current was not rapidly blocked by 20 µM RR. (E) Cold-sensitive current remained when 20 µM RR was included in both wash and cold perfusion buffers. (F) Delocalization of cold- and 2-APB–evoked currents. Cold-sensitive current ran down after initial activation, whereas 2-APB–sensitive current remained. (G) Current response activated by heat in *Xenopus* oocytes expressing frog TRPV3. Bottom trace shows bath temperature change. (H) Inhibition of heat-evoked currents by 50 µM RR in oocytes. (I) Current response in control oocytes evoked by heat. (J) Temperature-response profiles of heat-activated currents from TRPV3-expressing oocytes. Each trace corresponds to an individual recording. (K) Statistic plot of average current from oocytes containing TRPV3 compared with RR-inhibited current and current of control oocytes. All currents were recorded at a holding potential of −60 mV. Error bars represent mean ± SEM.

activation was quite variable, ranging from 20 to 12°C (Fig. 5 B). Several factors might contribute to the variation of the activation threshold. Because the current was inactivated rapidly, the activation time course could depend on the cooling rate of the oocyte. In our experiment, the temperature of the oocyte was changed by manually perfusing the recording chamber with precooled solutions. Thus, the cooling rate could differ substantially between experiments. The regulation of the channel could also be a factor for the variation of the activation threshold. Despite the quantitative difference in the threshold, the characteristic inactivation of the current was quite consistent, suggesting that the currents resulted from a common origin.

To determine whether TRPV3 mediated the apparent cold-sensitive current, we tested the sensitivity to RR. The application of 20 µM RR sufficed to fully inhibit the 2-APB response (Fig. 5 C). The blockade also occurred rapidly, as soon as the perfusion buffer was switched. In contrast, the application of 20 µM RR did not produce a similar block on the cold-evoked current (Fig. 5 D). Instead, the current decayed at a much slower rate, similar to the time course of inactivation in the absence of RR. In a separate test, we included 20 µM RR in perfusion buffers (both cooling buffer and wash buffer) so that RR was always present during experimentation. However, this maneuver was also ineffective; the cold-evoked current was still persisted and remained to undergo strong inactivation as in the absence of RR (Fig. 5 E). Overall, in all tested oocytes (n = 13), we found that RR consistently failed to block the cold-sensitive current, whereas it had no problem inhibiting the 2-APB response. Thus, the currents evoked by 2-APB and cold had a differential sensitivity to RR block.

In addition to a different pharmacological profile, we also found that the cold- and 2-APB–evoked responses exhibited a certain degree of de-localizability in several recordings (n = 6). Fig. 5 F shows currents elicited by repeated cold and 2-APB stimulation in the same oocyte. Initial cold stimulation resulted in a large response. But the current tended to run down in the subsequent stimulation. The 2-APB response, on the other hand, could be evoked repeatedly. Notably, the 2-APB response persisted, even after the cold response rundown, suggesting that the currents evoked by 2-APB and cold also differed in the property of rundown.

Lastly, we examined whether the recombinant TRPV3 is heat sensitive in *Xenopus* oocytes. As reported previously (Saito et al., 2011), it was shown that the channel does not respond to heat when expressed in *Xenopus* oocytes. However, their tested temperature appeared to be <50°C, which is lower than the temperature threshold of the channel found in HEK293 cells. Thus, we have examined the heat sensitivity of the channel over a higher temperature range >50°C. As illustrated in Fig. 5 G, a robust heat response was indeed detected in this temperature range from oocytes injected with frog TRPV3 transcript. Fig. 5 J plots the temperature activation profile, which shows that heat >50°C resulted in a rapidly increasing current. This temperature threshold in oocytes appears lower than but is still in the range of the activation threshold of the channel in HEK cells. The heat-evoked current in oocytes was also sensitive to RR (Fig. 5, H and K), further indicating that it was mediated by TRPV3. Consistently, the control oocytes that were not injected with TRPV3 exhibited negligible responses in a similar temperature range (Fig. 5, I and K). These data suggest that frog TRPV3 is also heat sensitive in *Xenopus* oocytes, indicating that its temperature sensitivity does not depend on cell types.

Endogenous cold sensitivity of *Xenopus* oocytes

The insensitivity of the cold-sensitive current to RR raises the question of whether the apparent cold response in the TRPV3-expressing oocytes was mediated by the channel. To address the problem, we further examined the cold sensitivity of control oocytes. Fig. 6 (A and B) shows that the control oocyte, whether injected or not, indeed expressed a cold-sensitive current. The size of the current varied between oocytes, with a mean of 1.33 ± 0.21 µA (n = 35). The current resembled that seen in TRPV3-injected oocytes in several aspects. First, it exhibited similar strong inactivation during cooling. Second, it also tended to run down over repeated activation (Fig. 6, A and C). Third, it was not blocked by RR

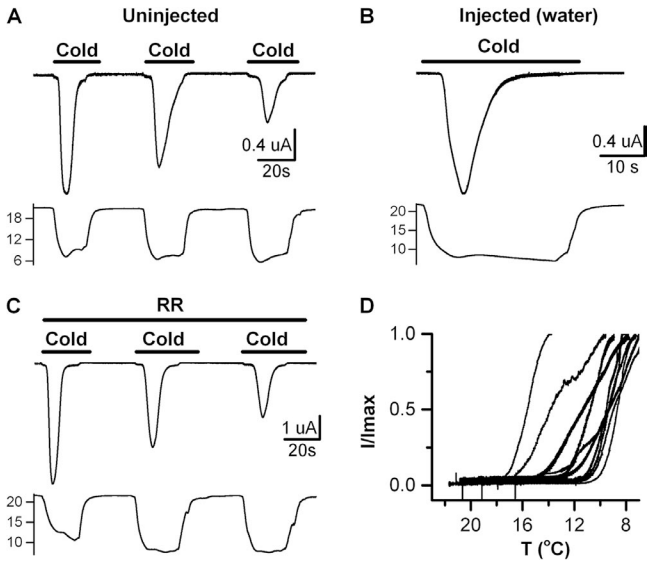

Figure 6. Endogenous cold responses in *Xenopus* oocytes. (A and B) Cold-sensitive currents recorded in control oocytes (A, uninjected; B, injected with water). (C) Endogenous cold-sensitive current was insensitive to RR block. Both wash and cooling buffers contained 20 µM RR. (D) Cold-response profiles of endogenous cold activity, showing similarly variable temperature activation thresholds as observed in frog TRPV3–expressing oocytes. All currents were recorded at a holding potential of −60 mV.

(Fig. 6 C). Fourth, its temperature responsiveness range overlapped with the current observed in TRPV3-expressing oocytes (Fig. 6 D). These similar characteristics suggest that the current expressed by control oocytes probably had the same origin as the cold-sensitive current observed in oocytes injected with frog TRPV3.

DISCUSSION

We have cloned and functionally expressed the western clawed frog TRPV3 in HEK293 cells. The heterologously expressed channels are activated by heat and 2-APB, two common stimuli for mammalian vanilloid receptors. The heat activation has a relatively high temperature threshold, >50°C. The temperature response has steep temperature dependence, with a temperature coefficient Q_{10} of ~71, which is equivalent to an enthalpy change of 93 kcal/mol between closing and opening. Both heat and 2-APB responses are profoundly sensitized over repeated stimulation. The sensitized channel even became responsive to warm temperatures. Cold evoked no detectable response with temperature as low as 5°C. The heat sensitivity of the channel was retained in excised patches. These basic functional characteristics of frog TRPV3, albeit with subtle changes such as a higher temperature activation threshold, are similar to those of mammalian TRPV3, suggesting that the frog orthologue is intrinsically heat sensitive.

A previous study by Saito et al. (2011) suggested that frog TRPV3, when expressed in *Xenopus* oocytes, responds to noxious cold. To test the possibility that the cold sensitivity of the channel may be dependent on cell types, we have also examined its function in *Xenopus* oocytes. Consistent with this previous report, large cold responses could be detected in oocytes expressing frog TRPV3. In addition, these cells also exhibit robust heat sensitivity. The heat response has similar characteristics of the current in mammalian cells, suggesting that the current is mediated by frog TRPV3. The previous study failed to detect heat sensitivity in *Xenopus* oocytes injected with frog TRPV3. The discrepancy is likely because temperature was elevated to only ~40°C in their study, which is still below the activation threshold of the channel. Although an apparent cold sensitivity appeared in TRPV3-expressing oocytes, our further examination revealed that the cold-evoked current had different characteristics than the current evoked by 2-APB or heat. For example, the cold-sensitive current was not blocked by RR, which is a common pore block of vanilloid receptors and thus would be expected to be effective if the current was conducted by frog TRPV3. The cold response was also inactivated rapidly, whereas the 2-APB and heat responses were sustained (in nominally Ca^{2+}-free solutions). Finally, the cold-sensitive current tended to run down over repeated activation. These different characteristics imply that the cold-sensitive current as observed in *Xenopus* oocytes could be mediated by a different channel or transporter other than TRPV3. In support of this possibility, we further found that control oocytes, whether they were injected (with water) or not, also expressed a cold-sensitive current. This endogenous current had all the characteristic properties of the cold-sensitive current observed in TRPV3-expressing oocytes, including strong inactivation, time-dependent rundown, and insensitivity to RR block. The endogenous current appeared to be somewhat smaller in size. But this difference could be explained by several hypotheses. For example, the expression of the endogenous cold-sensitive current was altered by the TRPV3 transcript, or alternatively, the endogenous cold receptors may be susceptible to interactions with TRPV3 proteins. Regardless of the quantitative difference in the current size, our experiments reveal that *Xenopus* oocytes possess an endogenous cold-sensitive current, which has the same properties of the current evoked by cold in oocytes heterologously expressing TRPV3.

Our finding of the heat sensitivity of frog TRPV3 is in agreement with another report on a truncated splice variant of the channel (Hu et al., 2009). Hu et al. showed that this splice variant of TRPV3 in *Xenopus tropicalis* lacks portions of N and C termini, so by itself it does not respond to either 2-APB or temperature. However, when the missing N- and C-terminal portions were added using the counterparts from mouse TRPV3, its function could be restored. The resulting chimera was also activated by heat in addition to 2-APB, similar to our observation of the heat sensitivity of the full-length frog TRPV3. These results are again consistent with an intrinsic heat sensitivity of the channel.

Xenopus oocytes have been widely used for electrophysiological study of thermal channels, including some with controversial cold sensitivity. However, it appears that there has been no report on endogenous cold sensitivity of the system. One possible reason is that the endogenous cold-sensitive current expressed by *Xenopus* oocytes have complex activation profiles, which could complicate the detection of the current. Because of rapid inactivation, the current may become small and therefore go undetected if cooling rate is too slow. Because of susceptibility to rundown, the appearance of the current could also be time dependent. For example, the previous report by Saito et al. (2011) showed that the cold-evoked current in TRPV3-expressing oocytes became suppressed during repeated stimulation in the presence of RR. This was interpreted as a blocking effect of RR and thus a key piece of evidence for attributing the current to frog TRPV3. However, the suppression of the current could also be caused by the rundown of the current instead of RR block. Conceivably, the occurrence of the current could also depend on buffer compositions and cell conditions. Because of

such variability, this endogenous cold sensitivity could be manifested in different ways. Our findings suggest that caution must be exercised for interpreting data obtained with such an expression system, especially for the study of cold-sensitive ion channels.

Despite the similar biophysical properties, frog TRPV3 shares with mammalian TRPV3 a limited sequence homology. For example, it has a sequence identity of ∼60% with mouse TRPV3. Thus, the frog TRPV3 is a distant orthologue of the mammalian counterpart. The key residues that control the channel functions, however, have apparently been conserved during evolution. Thus, the channel likely attains similar biological functions in different species. In mammals, the channel has been implicated in various physiological roles in hair growth, thermal sensation, skin barrier formation, itch, and so on. *Xenopus tropicalis* frogs have different characteristics in some of these functions and would provide an alternative model for comparative studies to further understand the in vivo functions of TRPV3.

The authors would like to thank Drs. Randall Rasmusson and Mark Parker (State University of New York at Buffalo, Buffalo, NY) for their generous supplies of *Xenopus* oocytes.

This work was supported by grant R01 GM104521 from the National Institutes of Health.

The authors declare no competing financial interests.

Richard W. Aldrich served as editor.

Submitted: 4 June 2015
Accepted: 8 September 2015

REFERENCES

Bautista, D.M., J. Siemens, J.M. Glazer, P.R. Tsuruda, A.I. Basbaum, C.L. Stucky, S.E. Jordt, and D. Julius. 2007. The menthol receptor TRPM8 is the principal detector of environmental cold. *Nature.* 448:204–208. http://dx.doi.org/10.1038/nature05910

Caterina, M.J., M.A. Schumacher, M. Tominaga, T.A. Rosen, J.D. Levine, and D. Julius. 1997. The capsaicin receptor: a heat-activated ion channel in the pain pathway. *Nature.* 389:816–824. http://dx.doi.org/10.1038/39807

Caterina, M.J., T.A. Rosen, M. Tominaga, A.J. Brake, and D. Julius. 1999. A capsaicin-receptor homologue with a high threshold for noxious heat. *Nature.* 398:436–441. http://dx.doi.org/10.1038/18906

Caterina, M.J., A. Leffler, A.B. Malmberg, W.J. Martin, J. Trafton, K.R. Petersen-Zeitz, M. Koltzenburg, A.I. Basbaum, and D. Julius. 2000. Impaired nociception and pain sensation in mice lacking the capsaicin receptor. *Science.* 288:306–313. http://dx.doi.org/10.1126/science.288.5464.306

Chowdhury, S., B.W. Jarecki, and B. Chanda. 2014. A molecular framework for temperature-dependent gating of ion channels. *Cell.* 158:1148–1158. http://dx.doi.org/10.1016/j.cell.2014.07.026

Clapham, D.E., and C. Miller. 2011. A thermodynamic framework for understanding temperature sensing by transient receptor potential (TRP) channels. *Proc. Natl. Acad. Sci. USA.* 108:19492–19497. http://dx.doi.org/10.1073/pnas.1117485108

Davis, J., J. Gray, M. Gunthorpe, J. Hatcher, P. Davey, P. Overend, J. Latcham, C. Clapham, K. Atkinson, K. Rance, et al. 2000. Abolition of hyperalgesia, but not algesia, in mice lacking VR1. *Eur. J. Neurosci.* 12:171.

Dhaka, A., A.N. Murray, J. Mathur, T.J. Earley, M.J. Petrus, and A. Patapoutian. 2007. TRPM8 is required for cold sensation in mice. *Neuron.* 54:371–378. http://dx.doi.org/10.1016/j.neuron.2007.02.024

Gau, P., J. Poon, C. Ufret-Vincenty, C.D. Snelson, S.E. Gordon, D.W. Raible, and A. Dhaka. 2013. The zebrafish ortholog of TRPV1 is required for heat-induced locomotion. *J. Neurosci.* 33:5249–5260. http://dx.doi.org/10.1523/JNEUROSCI.5403-12.2013

Gracheva, E.O., N.T. Ingolia, Y.M. Kelly, J.F. Cordero-Morales, G. Hollopeter, A.T. Chesler, E.E. Sánchez, J.C. Perez, J.S. Weissman, and D. Julius. 2010. Molecular basis of infrared detection by snakes. *Nature.* 464:1006–1011. http://dx.doi.org/10.1038/nature08943

Hu, H., J. Grandl, M. Bandell, M. Petrus, and A. Patapoutian. 2009. Two amino acid residues determine 2-APB sensitivity of the ion channels TRPV3 and TRPV4. *Proc. Natl. Acad. Sci. USA.* 106:1626–1631. http://dx.doi.org/10.1073/pnas.0812209106

Jara-Oseguera, A., and L.D. Islas. 2013. The role of allosteric coupling on thermal activation of thermo-TRP channels. *Biophys. J.* 104:2160–2169. http://dx.doi.org/10.1016/j.bpj.2013.03.055

Kindt, K.S., V. Viswanath, L. Macpherson, K. Quast, H. Hu, A. Patapoutian, and W.R. Schafer. 2007. *Caenorhabditis elegans* TRPA-1 functions in mechanosensation. *Nat. Neurosci.* 10:568–577. http://dx.doi.org/10.1038/nn1886

Liu, B., J. Yao, M.X. Zhu, and F. Qin. 2011. Hysteresis of gating underlines sensitization of TRPV3 channels. *J. Gen. Physiol.* 138:509–520. http://dx.doi.org/10.1085/jgp.201110689

Majhi, R.K., A. Kumar, M. Yadav, N. Swain, S. Kumari, A. Saha, A. Pradhan, L. Goswami, S. Saha, L. Samanta, et al. 2013. Thermosensitive ion channel TRPV1 is endogenously expressed in the sperm of a fresh water teleost fish (*Labeo rohita*) and regulates sperm motility. *Channels (Austin).* 7:483–492. http://dx.doi.org/10.4161/chan.25793

McKemy, D.D., W.M. Neuhausser, and D. Julius. 2002. Identification of a cold receptor reveals a general role for TRP channels in thermosensation. *Nature.* 416:52–58. http://dx.doi.org/10.1038/nature719

Moqrich, A., S.W. Hwang, T.J. Earley, M.J. Petrus, A.N. Murray, K.S. Spencer, M. Andahazy, G.M. Story, and A. Patapoutian. 2005. Impaired thermosensation in mice lacking TRPV3, a heat and camphor sensor in the skin. *Science.* 307:1468–1472. http://dx.doi.org/10.1126/science.1108609

Ohkita, M., S. Saito, T. Imagawa, K. Takahashi, M. Tominaga, and T. Ohta. 2012. Molecular cloning and functional characterization of *Xenopus tropicalis* frog transient receptor potential vanilloid 1 reveal its functional evolution for heat, acid, and capsaicin sensitivities in terrestrial vertebrates. *J. Biol. Chem.* 287:2388–2397. http://dx.doi.org/10.1074/jbc.M111.305698

Peier, A.M., A. Moqrich, A.C. Hergarden, A.J. Reeve, D.A. Andersson, G.M. Story, T.J. Earley, I. Dragoni, P. McIntyre, S. Bevan, and A. Patapoutian. 2002a. A TRP channel that senses cold stimuli and menthol. *Cell.* 108:705–715. http://dx.doi.org/10.1016/S0092-8674(02)00652-9

Peier, A.M., A.J. Reeve, D.A. Andersson, A. Moqrich, T.J. Earley, A.C. Hergarden, G.M. Story, S. Colley, J.B. Hogenesch, P. McIntyre, et al. 2002b. A heat-sensitive TRP channel expressed in keratinocytes. *Science.* 296:2046–2049. http://dx.doi.org/10.1126/science.1073140

Prober, D.A., S. Zimmerman, B.R. Myers, B.M. McDermott Jr., S.H. Kim, S. Caron, J. Rihel, L. Solnica-Krezel, D. Julius, A.J. Hudspeth, and A.F. Schier. 2008. Zebrafish TRPA1 channels are required for chemosensation but not for thermosensation or mechanosensory hair cell function. *J. Neurosci.* 28:10102–10110. http://dx.doi.org/10.1523/JNEUROSCI.2740-08.2008

Qin, F. 2013. Demystifying thermal channels: Driving a channel both forwards and backwards with a single gear? *Biophys. J.* 104:2118–2120. http://dx.doi.org/10.1016/j.bpj.2013.04.017

Saito, S., N. Fukuta, R. Shingai, and M. Tominaga. 2011. Evolution of vertebrate transient receptor potential vanilloid 3 channels: Opposite temperature sensitivity between mammals and western clawed frogs. *PLoS Genet.* 7:e1002041. http://dx.doi.org/10.1371/journal.pgen.1002041

Smith, G.D., M.J. Gunthorpe, R.E. Kelsell, P.D. Hayes, P. Reilly, P. Facer, J.E. Wright, J.C. Jerman, J.P. Walhin, L. Ooi, et al. 2002. TRPV3 is a temperature-sensitive vanilloid receptor-like protein. *Nature.* 418:186–190. http://dx.doi.org/10.1038/nature00894

Spray, D.C. 1986. Cutaneous temperature receptors. *Annu. Rev. Physiol.* 48:625–638. http://dx.doi.org/10.1146/annurev.ph.48.030186.003205

Viswanath, V., G.M. Story, A.M. Peier, M.J. Petrus, V.M. Lee, S.W. Hwang, A. Patapoutian, and T. Jegla. 2003. Opposite thermosensor in fruitfly and mouse. *Nature.* 423:822–823. http://dx.doi.org/10.1038/423822a

Watanabe, H., J. Vriens, S.H. Suh, C.D. Benham, G. Droogmans, and B. Nilius. 2002. Heat-evoked activation of TRPV4 channels in a HEK293 cell expression system and in native mouse aorta endothelial cells. *J. Biol. Chem.* 277:47044–47051. http://dx.doi.org/10.1074/jbc.M208277200

Xu, H., I.S. Ramsey, S.A. Kotecha, M.M. Moran, J.A. Chong, D. Lawson, P. Ge, J. Lilly, I. Silos-Santiago, Y. Xie, et al. 2002. TRPV3 is a calcium-permeable temperature-sensitive cation channel. *Nature.* 418:181–186. http://dx.doi.org/10.1038/nature00882

Xu, H., M. Delling, J.C. Jun, and D.E. Clapham. 2006. Oregano, thyme and clove-derived flavors and skin sensitizers activate specific TRP channels. *Nat. Neurosci.* 9:628–635. http://dx.doi.org/10.1038/nn1692

Yao, J., B. Liu, and F. Qin. 2009. Rapid temperature jump by infrared diode laser irradiation for patch-clamp studies. *Biophys. J.* 96:3611–3619. http://dx.doi.org/10.1016/j.bpj.2009.02.016